Assessment of the Effect of Dual Impeller Alignment on the Heat Transfer Coefficient in Stirred Tanks

Ruben Ramírez-Gómez[a], Sergio A. Martínez-Delgadillo[a], Daniel García-Cortés[b], Helvio R. Mollinedo-Ponce[c], Oliver M. Huerta-Chávez[d], Jorge Ramírez-Muñoz[a],[*]

[a]División de Ciencias Básicas e Ingeniería, Universidad Autónoma Metropolitana Unidad Azcapotzalco. Av. San Pablo 180, Col. Reynosa Tamaulipas, Azcapotzalco, D.F. 02200, Mexico
[b]Instituto Superior de Tecnologías y Ciencias Aplicadas (InSTEC), Quinta de los Molinos, Ave. Salvador Allende y Luaces, Plaza de la Revolución, Ciudad de La Habana, Cuba
[c]UPIITA, Instituto Politécnico Nacional. Av. IPN 2580, Ticoman. México D.F.
[d]SEPI ESIME Ticoman. Instituto Politécnico Nacional. Av San Jose Ticoman, La Laguna Ticoman. G.A. Madero, 07340, México .D.F.
jrm@correo.azc.uam.mx

Chemical processes usually rely on mechanically stirred tanks to perform several operations in sequential or simultaneous manner. Existing correlations for local heat transfer coefficient estimation are valid only for specific geometrical configurations and most academic works regard the so-called standard geometry using only one impeller. However, many industrial tanks operate with two or more impellers whose alignment has been rarely studied previously. In this work, we study the effect of impeller alignment (phase angle) in the local heat transfer coefficient (h_i) for lab-scale heating experiments in a stirred cylindrical tank (turning anti clockwise) equipped with two high-efficiency impellers (HE3) and two pitched blade impellers (PB4). It was found that a 0° phase angle yields higher values of h_i for the HE3 impellers, i.e., this configuration is more efficient for heat transfer purposes than its counterpart with a 60° phase angle. No significant effect was observed by varying the aligned between impellers for the case of pitched blade impellers. In addition, Computational Fluid Dynamics (CFD) analysis was used to evaluate the hydrodynamic inside the tank for the four different impeller configurations. It was observed a more efficient synchronization of the pumping loops generated by both impellers with 0° phase angle between impellers.

1. Introduction

Cylindrical mechanically agitated tanks are widely used in the chemical process industries, either in continuous, batch or semi-batch operations. Therefore, theoretical and experimental studies of these systems remain a topic of current interest. The performance of a stirred tank depends largely on the characteristics of pattern flow and turbulent intensity induced by an impeller (Paul et al., 2004). For this reason, several recent works have been focused on identifying the characteristics of pattern flow generated by different impeller types and its relationship with important design parameters like power consumption (Molnár et al., 2013), baffles effect in the multi-phase flow structure inside a reactor (Zhang et al., 2013), angular speed effect in the homogeneity of flow velocity field, turbulence intensity and reaction time in a electrochemical reactor used to remove hexavalent chromium from industrial wastewaters (Martínez-Delgadillo et al., 2013). On the other hand, in some applications - e.g. highly exothermic reactions -, temperature control is the most important factor for process operability and safety. Therefore, the ability for remove heat can be quite critical in these systems and the characterization of the system's heat removal capacity is of paramount importance. In this work, the heat transfer at the wall of an agitated vessel with a dished bottom and four equally spaced baffles was investigated. Two well-known dual impeller types were studied: i) the high-efficiency impeller (HE3), and ii) the pitched-blade turbine with four

45° inclined blades (PB4). The ratio of impeller diameter (D) to the impeller blade width (W) for both impellers was maintained constant, i.e. $D/W=5$.

Heat removal capacity depends mainly on the overall heat transfer coefficient U, which is defined by (Kern, 1950)

$$\frac{1}{U} = \frac{1}{h_i} + ff_i + \frac{x}{k} + ff_j + \frac{1}{h_j} .$$

(1)

Where:
- h_i: Process side local heat transfer coefficient, W/m^2 ^{o}C.
- ff_i , ff_j: Process and service side fouling factors, m^2 ^{o}C/W.
- x, k: Wall thickness and its conductivity, m and W/m ^{o}C.
- h_j: Service side local heat transfer coefficient, W/m^2 ^{o}C.

In most cases, h_i is the limiting resistance to heat transfer, and it is a function of the specific stirring system geometry, the operating conditions, and the fluid properties. In the in the scientific literature (e.g. Bondy and Lippa, 1983) or in textbooks (e.g. McKetta, 1992), it is common to find local heat transfer correlations for stirred tanks using several single impeller geometries with the so-called standard geometry. However, the characterization of the heat removal capacity of stirred tanks with multiple impellers has received little attention in the literature. Additionally, according to our knowledge of the literature, the effect of varying the alignment between impellers in the local heat transfer coefficient has not been previously studied. In this work, process side heat-transfer coefficients for heating experiments in a stirred tank were determined using two different pairs of impellers. Experimental and numerical studies have been carried out to evaluate the effect of impeller alignment -rotating counter clockwise- in the local heat transfer coefficient and in the field velocity around the impellers.

2. Materials and methods

2.1 Experimental equipment and materials

Tests were carried out in a cylindrical stirred vessel turning anti clockwise, whose capacity was 2 L and inside diameter $T=132$ mm (Figure 1). The impeller diameter used was $D=64$ mm, and the mass of the process fluid was M=2.411 kg (liquid height $Z=155$ mm). The process fluid was prepared with a solution glycerin/water (80 % glicerina and 20 % water). The variation range of the viscosity (μ) and density (ρ) of the process fluid during the experiments were from 4.535×10^{-2} Pa-s and 1207.89 kg/m^3 (25 ^{o}C) to 4.444×10^{-3} Pa-s and 1,170.88 kg/m^3, (75 ^{o}C). As can be seen in Figure 1, the temperature data during the experiments were recorded using a data acquisition system (FieldPoint). Meanwhile, the fluid service temperature was maintained constant (with a variation of ± 1 ^{o}C) by using a temperature bath.
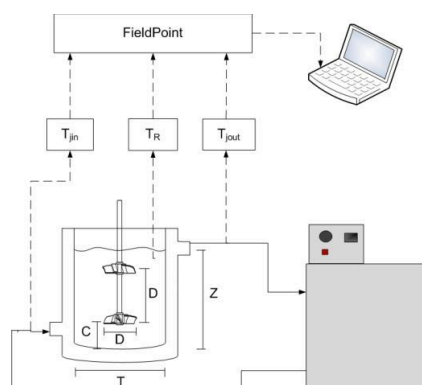

Figure 1: Experimental system with vessel details.

2.2 Heat transfer coefficient model

In order to simplify the analysis, the following assumptions were made: 1) there are no heat losses to the environment (adiabatic system), 2) the process fluid and vessel temperature are equal, 3) the energy injection due to agitation is negligible, 4) the evolution of the service fluid temperature in the jacket follows a logarithmic trajectory (fluid service non-isothermal), and 5) the physical properties of the process fluid and service remain constant in the temperature range in which the heat transfer coefficient is evaluated (5 ^{o}C). For this case, the heat global coefficient for heating experiments can be estimated from (Kern, 1950)

$$ln\left[\frac{T_{R_0} - T_{jin}}{T_R - T_{jin}}\right] = \left[\frac{w\,c}{C_{pm}}\right]\left[\frac{K-1}{K}\right]\theta \;. \tag{2}$$

Where:

$K = e^{(UA/wc)}$: Dimensionless constant.

T_{R0}: Process fluid temperature at the initial time, ^{o}C.

T_{jin}: Inlet temperature of the fluid service, ^{o}C.

T_{jout}: Outlet temperature of the fluid service, ^{o}C.

θ: Elapsed time in the temperature range in which the heat transfer coefficient is evaluated, s.

w: Mass flow of the service fluid, kg/s.

C_{pm}: Is the sum of the heat capacity of the process fluid, vessel, stirrers and baffles multiplied by their respective masses, J/^{o}C.

c: Heat capacity of the service fluid, J/kg ^{o}C.

Thus, a regression of $ln\left[T_{R_0} - T_{jin}/T_R - T_{jin}\right]$ versus time θ should produce a straight line with slope $\left[w\,c/C_{pm}\right]\left[K-1/K\right]$. Using the known values for A, w, C_{pm} and c, the overall heat transfer coefficient U can be estimated.

2.3 Wilson method

The Wilson´s (1915) method for estimating h_i comprises the following steps:

    1) The global transfer coefficient given in Eq(1) is rewritten as:

$$\frac{1}{U} = \frac{1}{h_i} + \frac{1}{h^*} \;, \tag{3}$$

where $1/h^*$ includes all the resistances not considered in $1/h_i$.

    2) The Sieder-Tate correlation is rewritten as:

$$h_i = \alpha k/D\;Re^{2/3}Pr^{1/3}\left(\mu/\mu_w\right)^{0.14} = \beta N^{2/3} \;. \tag{4}$$

Where α, and k are constants to be determined in the correlation and the fluid conductivity in the process fluid side, respectively. Furthermore, $Re = ND^2\rho/\mu$, $Pr = C_p\mu/k$ and $Nu = h_i\,D/k$ are the Reynolds number, the Prandtl number and the Nusselt number.

    3) Using Eq(4) in Eq(3) it is obtained

$$\frac{1}{U} = \frac{1}{\beta N^{2/3}} + \frac{1}{h^*} \tag{5}$$

Therefore, by performing experiments for different N values, when plotting $1/U$ vs $N^{-2/3}$ for each temperature range, and extrapolating when $N^{-2/3}\to 0$, it is possible to estimate $1/h^*$. Knowing $1/U$ and $1/h^*$, $1/h_i$ is obtained by using Eq (3). The determination of fluid physical properties in Eq(5) was estimated using correlations of the literature and considering the water-glycerin mixture as an ideal solution.

3. Results and discussions

3.1 Local heat transfer coefficient

Figure 2a and 2b shows the experimental data fitting for heating experiment using HE3 impellers with an existing Sieder-Tate correlation. As can be seen, the slope value for the aligned impellers, i.e. its h_i value is 10 % higher compared to non-aligned impellers. This same comparison was realized for PB4 stirrers (which is not shown), and the obtained values of the slope was 0.508 (PB4 non-aligned) and 0.511 (PB4-aligned). Therefore, its difference is less than 1 %. These results suggest that the alignment between impellers has a higher effect on the heat transfer coefficient (h_i) for HE3 impellers than for PB4. Thus, a 0° phase angle yields higher values of h_i, i.e., this configuration is more efficient for heat transfer purposes than its counterpart with a 60° phase angle when h_i is the limiting resistance to heat transfer. This phenomenon can be associated to a more efficient synchronization of the pumping loops generated by both impellers with 0° phase angle and will be discussed in detail below.
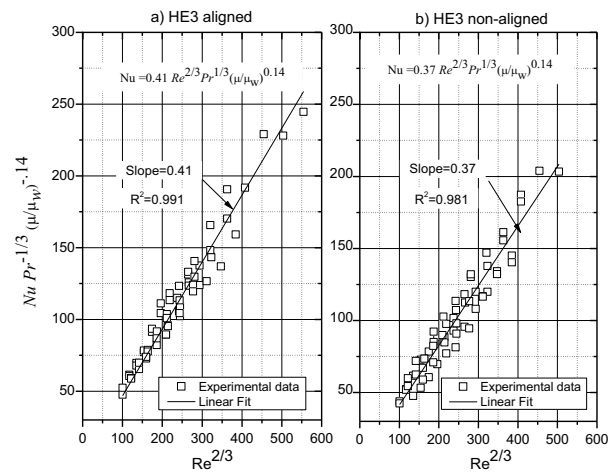
Figure 2: Sieder-Tate correlation for dual impeller (HE3) and heating experiments a) aligned, b) non-aligned.

3.2 CFD simulations

The related CFD model of the stirred tank was prepared to analyze its performance at different agitation rate: 300, 600 and 900 rpm. The continuity and momentum equations were solved using the commercial software Fluent, 6.3.26. Several types of meshing were included in order to obtain independent results from the numerical parameters. Furthermore, an adaptive mesh refinement scheme was useful to ensure grid independence. Details of the numerical solution can be found in a recently published paper (Martínez-Delgadillo et al., 2013). To evaluate the modifications induced on the flow for the two different alignments between impellers (0° and 45° for PB4, and 0° and 60° for HE3), Figures 3 and 4 shows the field velocity around the impellers turning anti clockwise for 300 and 900 rpm. As can be seen in Figures 3a-b and Figures 4a-b, for PB4 impellers, two short circuit flows above the upper impeller appear as a result of vary the alignment between impellers. Meanwhile for HE3 impellers (Figures 3c-d and Figures 4c-d), it is observed that, only one short circuit flow appears.
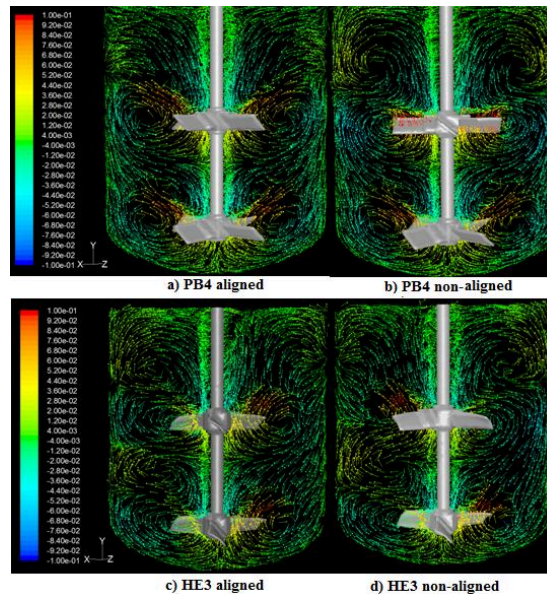

Figure 3: Effect of impellers alignment for dual impeller systems for 300 rpm (Re=545).

Because a strong top-to-bottom flow provides good uniformity and enhances the transference heat rate, the onset of short circuit flows explains why the local heat transfer coefficient decreases for non-aligned impellers.
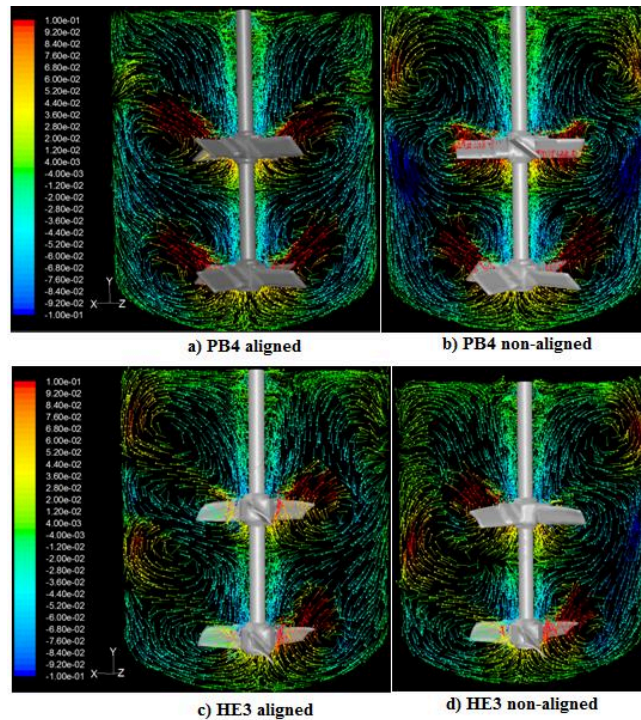

Figure 4: Effect of impellers alignment for dual impeller systems for 900 rpm (Re=1636).

For processes limited by pumping (e.g. heat transfer), the volumetric flow discharged from an impeller (Q) are used to evaluate the overall mixing efficiency. Traditionally, the effectiveness of an impeller can be defined as the impeller capacity of maximise Q for a given energy dissipation rate (ε) or power injected (εM) (Nienow, 1997), which is equivalent to minimise the power consumption for a Q. In order to compare the efficiency of each configuration tested in this work, the volumetric flow circulating between the impellers across the cross sectional area of the vessel were estimated (see Figure 5).
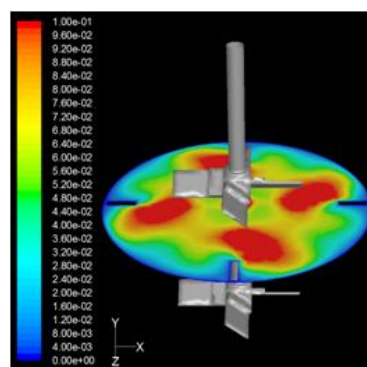

Figure 5: Velocity field between the PB4 aligned impellers for 600 rpm (Re=1091).

In Table 1 are shown the flow efficiency parameter for 600 rpm (Re=1091). As can be seen, according of this efficiency parameter, the non-aligned impellers are more effective than the aligned impellers. However, according to our experimental results, the alignment impellers are more efficient for heat transfer purposes than its counterpart non-alignment configuration. Thus, these results suggest that this flow efficiency parameter may not be so simply connected if there are short circuit flows.

Table 1: Flow efficiency parameter for 600 rpm (Re=1091).

	PB4 aligned	PB4 non-aligned	HE3 aligned	HE3 non-aligned
$\varepsilon \ (m^2s^{-3})$	0.3596974	0.3647725	0.2316276	0.2351394
$Q \ (m^3s^{-1})$	0.0008514	0.0008757	0.0006417	0.0006918
$M\varepsilon/Q \ (Wm^{-3}s)$	1,018.63	1,004.38	870.31	819.57

4. Conclusions

Varying the alignment between high efficiency impellers (HE3), i.e. phase angle from 0° to 60°, decreased the local heat transfer coefficient by 10 %. However, no important difference was obtained when the alignment between pitched blade turbines (PB4) was modified, phase angle from 0° to 45°. In order to understand why the alignment impellers are more efficient for heat transfer purposes than its counterpart non-alignment configuration, CFD simulations were performed using the commercial software Fluent. The flow velocity field around impellers were evaluated for depicting the hydrodynamic behaviour inside the tank at two different flow regimes: *Re*=545 and *Re*=1,636. It was found that although the non-alignment impellers are more efficient to maximise the volumetric flow circulating between the impellers for a given injected power, a short circuiting flow (reversed flow) appears above the upper impeller. Because the heat transfer is a flow controlled operation (i.e. limited by pumping), as a result of this reverse flow, for the case of non-alignment impellers (PB4 and HE3), both, the top-to-bottom turnover flow and the local heat transfer coefficient decreases.

References

Bondy F., Lippa S., 1983, Heat transfer in Agitated Vessels, Chem. Eng. Sci., 90(7), 62-71.

Kern D.Q., 1950, Process Heat Transfer. McGraw-Hill Book Co., New York, USA.

Martínez-Delgadillo, S.A., Ramírez-Muñoz, J., Mollinedo, H.R., Mendoza-Escamilla, V., Gutiérrez-Torres, C,.Jiménez-Bernal, J, 2013, Determination of the Spatial Distribution of the Turbulent Intensity and Velocity Field in an Electrochemical Reactor by CFD. Int. J. Electrochem. Sci., 8,274-289.

McKetta J. J., 1992, Heat Transfer Design Methods. Marcel Dekker. New York, USA.

Molnár, B., Egedy, A., Varga, T. 2013, CFD Model Based Comparison of Mixing Efficiency of Different Impeller Geometries, Chemical Engineering Transactions, 32, 1441-1446.

Nienow A.W., 1997, On impeller circulation and mixing effectiveness in the turbulent flow regime. Chem. Eng. Sci. 52, 2557-2565.

Paul E. L., Atiemo-Obeng V. A., Kresta S. M. 2004, Handbook of Industrial Mixing Science and Practice. Wiley-Interscience, New Jersey, USA.

Wilson E.E., 1915, A Basis for Rational Design of Heat Transfer Apparatus, Trans. of the American Society of Mechanical Engineers, 37, 47-82.

Zhang, S., Müller, D., Arellano-Garcia, H., Wozny, G. 2013, CFD Simulation of the Fluid Hydrodynamics in a Continuous Stirred-Tank Reactor, Chemical Engineering Transactions, 32, 1441-1446.